Electron-Ion Collider, Thomas Jefferson National Accelerator Facility			
Doc No. EIC-DET-TN-006 JLAB-TN-24-020	**Author:** R. Rajput-Ghoshal	**Effective Date:** July 2, 2024	**Review Frequency:** n/a
Technical Note: EIC Central Detector (ePIC) - RCS Stray Field Reduction			**Version:** 2.0

Electron-Ion Collider

Technical Note

EIC Central Detector (ePIC) - RCS Stray Field Reduction

Submitted by:

Renuka Rajput-Ghoshal
Renuka Rajput-Ghoshal (Jul 3, 2024 10:35 EDT)

Renuka Rajput-Ghoshal, Magnet Group
Experimental Nuclear Physics Division
Thomas Jefferson National Accelerator Facility

Reviewed by:

Sandesh Gopinath
Sandesh Gopinath (Jul 8, 2024 09:36 EDT)

Sandesh Gopinath, Magnet Group
Experimental Nuclear Physics Division
Thomas Jefferson National Accelerator Facility

Approved by:

Elke Aschenauer
Elke Aschenauer (Jul 3, 2024 20:15 EDT)

Elke Aschenauer, Detector Systems
Electron-Ion Collider
Brookhaven National Laboratory

Rolf Ent
Rolf Ent (Jul 3, 2024 10:38 EDT)

Rolf Ent, Detector Systems
Electron-Ion Collider
Thomas Jefferson National Accelerator Facility

VERSION HISTORY

Version #	Effective Date	Reviewer(s)	Summary of Change
1.0	6/20/2024	Renuka Rajput-Ghoshal	Initial EIC Tech Note
2.0	07/02/2024	Sandesh Gopinath	• Added Bx, By & Bz plots – Fig. 10-12 • Added longitudinal field integral along the RCS line for various length in the simulation model, Fig.13 • Added the text to explain Fig. 13 in discussion and conclusion section • Deleted a paragraph after Table 2, this was duplicated in the paragraph after Table 1

Introduction

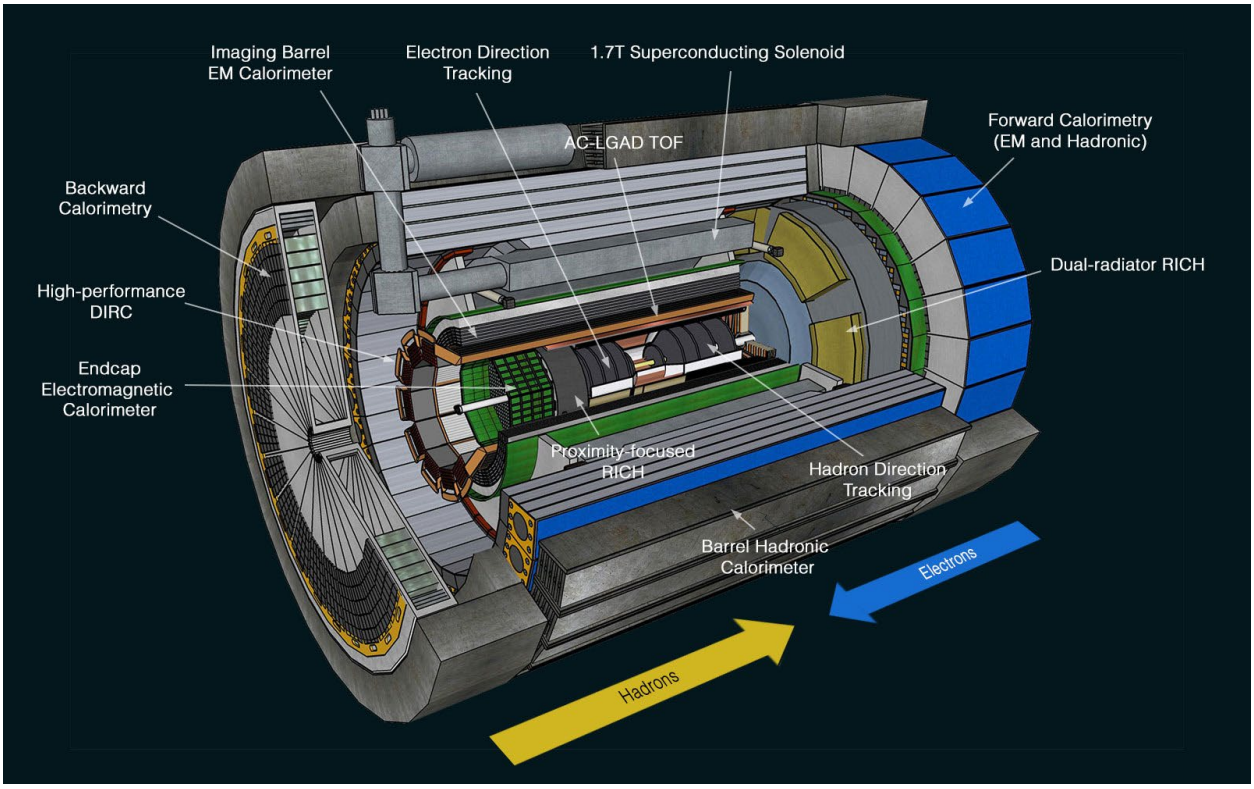

Figure 1 ePIC Detector Design schematic.

The Electron-Ion Collider (EIC) is a new accelerator currently build at Brookhaven National Laboratory (BNL) colliding beams of electrons and ions. This project is realized as a collaborative effort between BNL and Jefferson Lab (JLab) and scheduled to start operations in the early 2030s. The EIC General Purpose Detector system, ePIC (Fig. 1), is located at Interaction point 6 (IP6) and includes a 2T solenoid (MARCO) at its heart. The solenoid is 3.5 m in diameter and 3.8 m long, it will use a niobium-titanium conductor cooled at 4.5 K.

The magnet is surrounded by flux return steel, which includes the steel in the HCals (Hadronic Calorimeters), and additional steel was added to further reduce the stray field. The magnetic field is captured within the flux return steel with minimum leakage. Nevertheless, there are stray field requirements at IP6 that the electromagnetic design is required to adhere to. This document summarizes the various electromagnet studies completed in order to minimize the stray field at the Rapid Cycling Synchrotron beamline passing through IP6. OPERA/TOSCA [1] was used to perform electromagnetic field analysis with the complex flux return geometry simplified as primitive solid bodies.

Baseline configuration

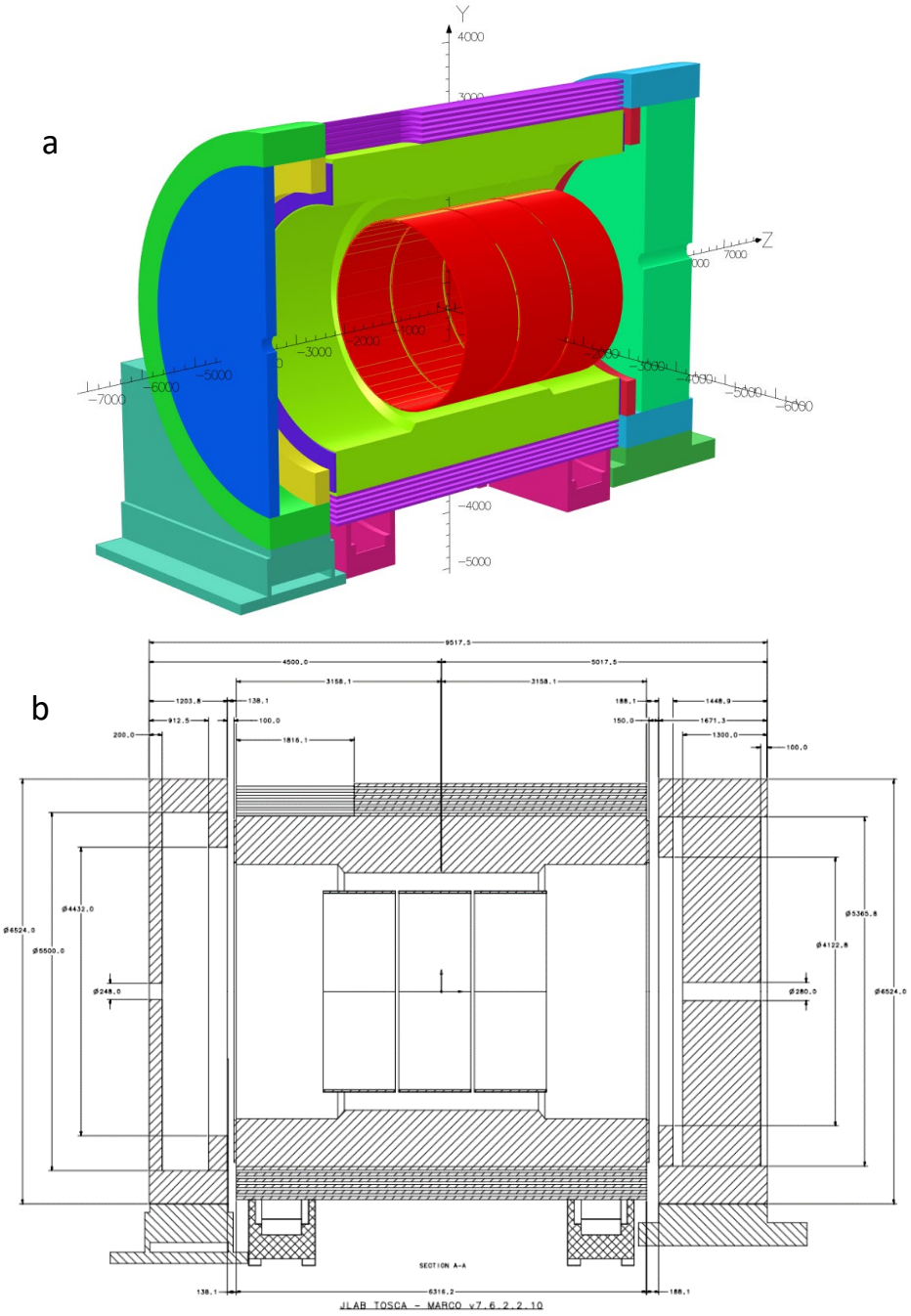

Figure 2 Simplified geometry that captures the soft magnetic steel – including steel in the subdetectors and steel used for shielding top: TOSCA model of the baseline geometry with the coils shown in red. Bottom: detailed dimensions with a cross section view of the implemented geometry.

Figure 2 shows the cross section view of the simplified flux return steel as modeled in TOSCA. The baseline geometry includes the flux return that is part of the Hadronic Calorimeters (HCals), magnetic shielding steel and the simplified endcap support structures that are made of steel as well.

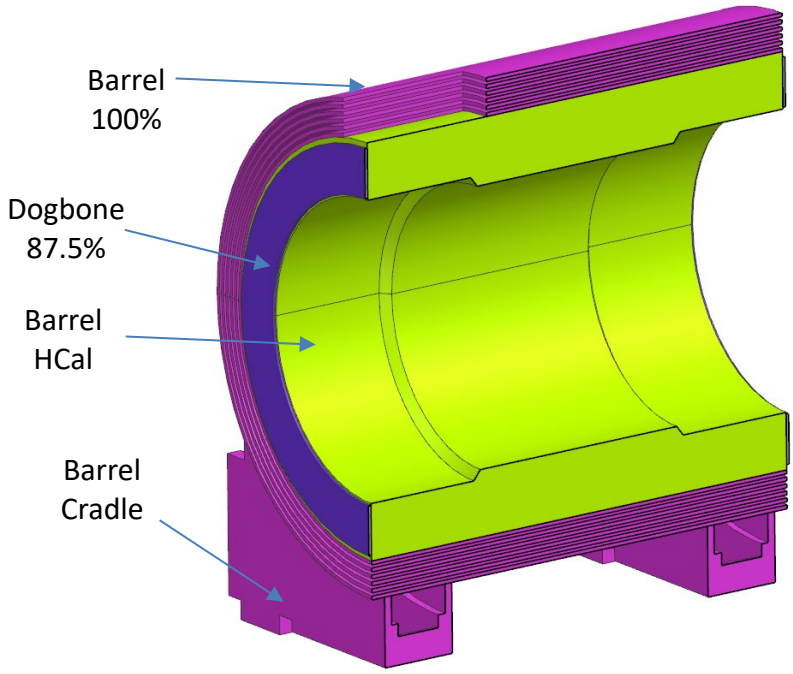

Figure 3 Electromagnetic nomenclature showing the Barrel Hadron calorimeter and the Barrel steel that is added for magnetic shielding.

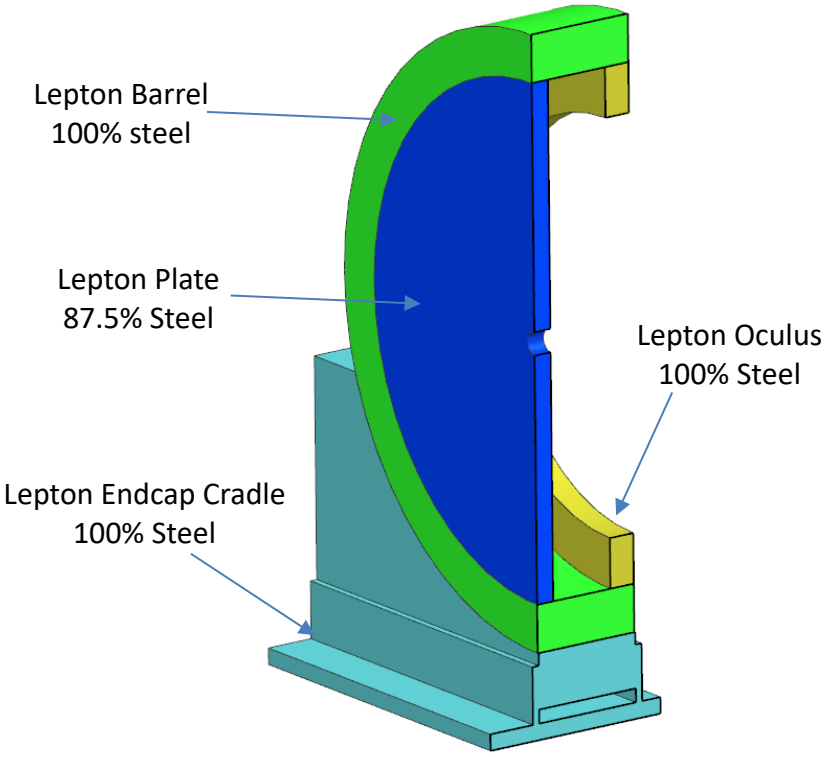

Figure 4 Electromagnetic nomenclature showing the Lepton/Backward Endcap assembly. All components were added for magnetic shielding.

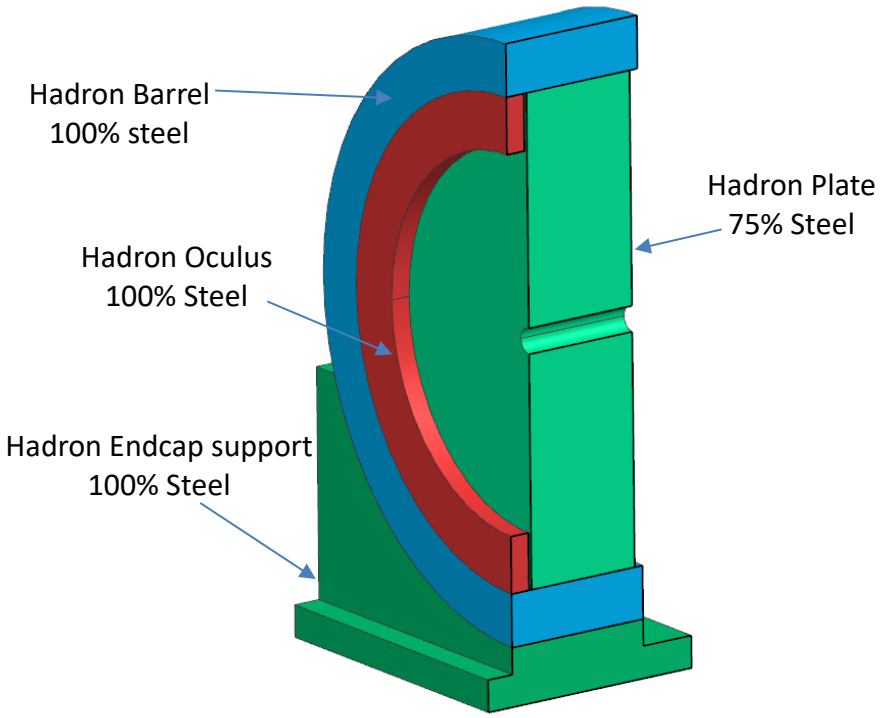

Figure 5 Electromagnetic nomenclature showing the Hadron/Forward Endcap assembly. The hadronic calorimetry were approximated as the Hadron plate, all components were added for magnetic shielding.

Table 1 Iron fraction in the HCal components [2]

Item	Iron fraction
Barrel Hadron Calorimeter	70%
Hadron Plate	75%
Lepton Plate	87.5%
Dogbones	66%
Barrel	100%
Hadron Barrel	100%
Lepton Barrel	100%
Cradles, Endcap supports	100%
Hadron Oculus	100%
Lepton Oculus	100%

All steel is considered to be 1020 steel. The geometries of detectors that have steel in them are simplified into larger primitive shapes by including the geometric voids and material voids left by presence of nonmagnetic materials. A dilution percentage is assigned to the components according to the average fraction of the ferromagnetic material in the total volume of the HCal steel (see Table 1.). These values are subject to minimal changes as the design of the detector and magnet flux return matures to incorporate manufacturing and other practical allowances. The revised naming convention for

electromagnetic simulation purposes are shown in Fig. 3, 4 & 5. Geometries with 100% iron are the steel added in addition to the existing steel in the detectors. Dogbones are 38.1 mm thick structural plates that are part of the Barrel Hcal.

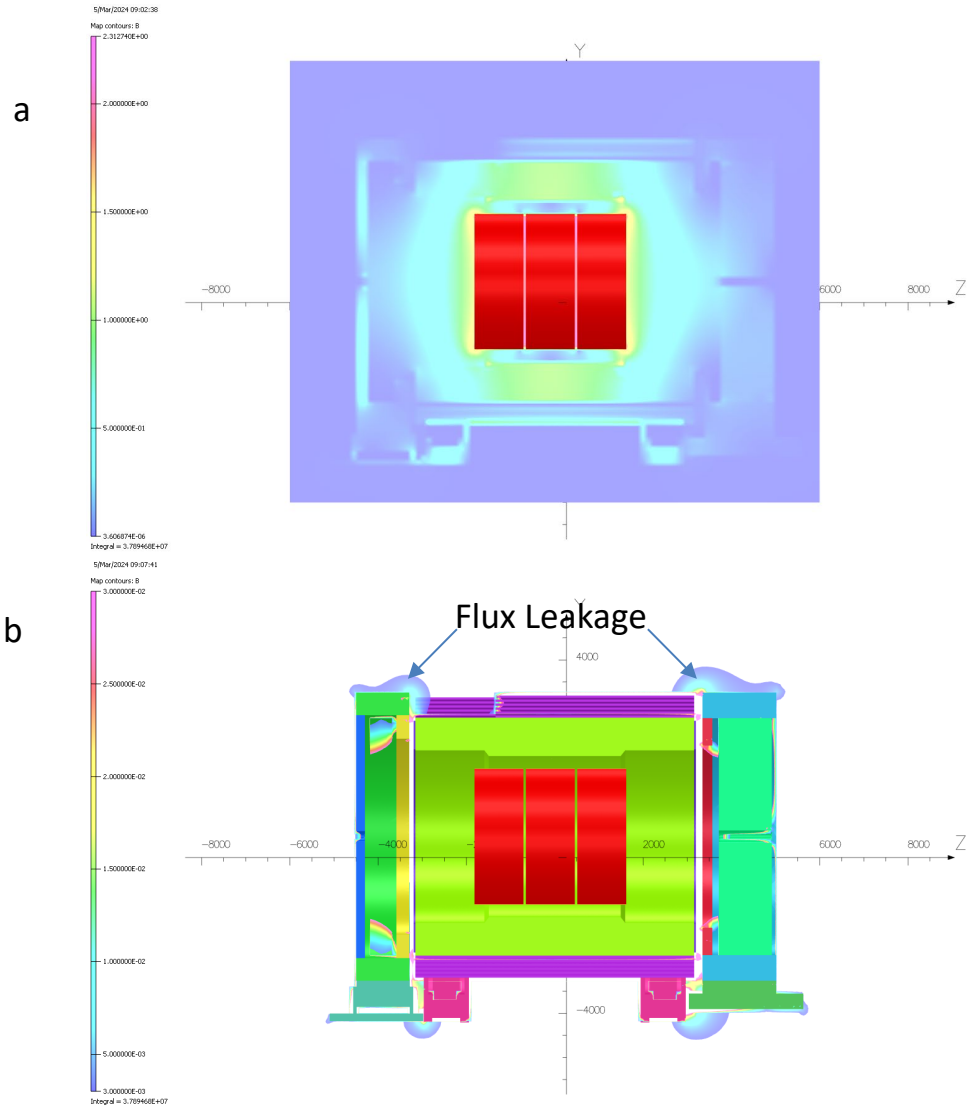

Figure 6 TOSCA field distribution for the baseline case with only the coils shown in red (top 9a)) and with the field capped off at a minimum of 30 Gauss and a maximum of 300 Gauss (Coils in red with steel in solid colors) (bottom (b)). Field leakages are primarily near the openings between the barrel and the endcap HCal.

Fig. 6a shows the TOSCA results with a field of order of 0.1 T (1000 Gauss) captured within the steel. Flux leakages of less than 300 Gauss are seen near the gaps between the barrel HCal and the endcap HCal (Fig. 6b).

a

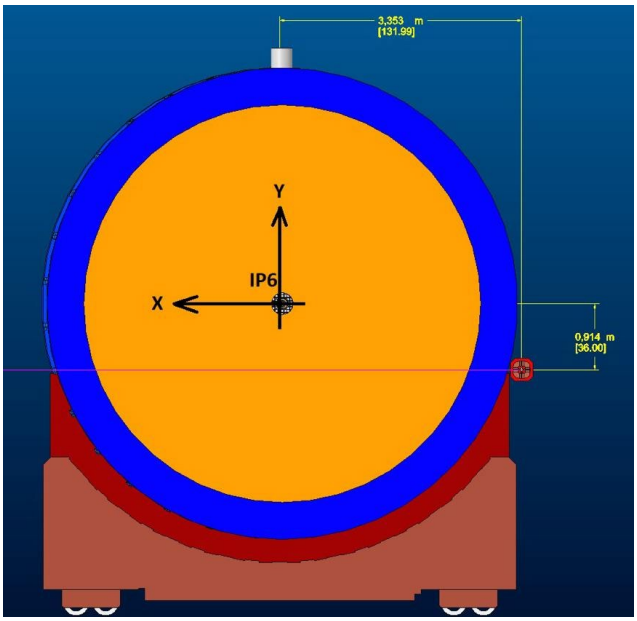

b

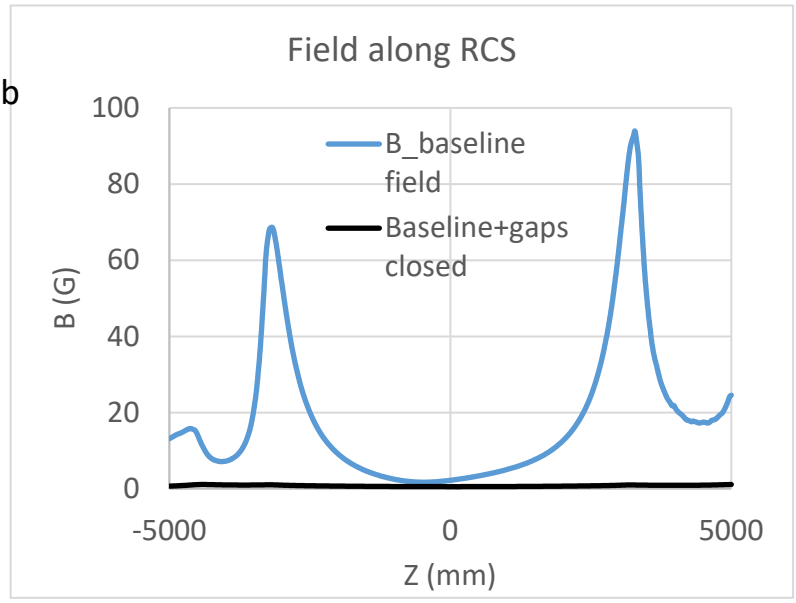

Figure 7 a. RCS location: x=3.353 m, y=-0.914 mm, z=-5 m to 5 m b. Stray field plot for the baseline case

The Rapid Cyclotron Synchrotron (RCS) beamline is approximately 3.5 m radially away from the IP6 center (Fig. 7). The stray field limit for along the RCS beamline of <0.007 T-m was placed to limit the polarized electron beam loss [3]. Instead of defining the field along the full length of the magnet, we converted this specification further in to field at location (3400, 0, 0) < 10G. There was no separate specification given for the maximum field along the RCS, so we assumed that a uniform 10G. The peak stray field is on the order of 100 Gauss with the total field integral of 0.0187 Tm along the RCS (Fig. 7b). The flux leakage is through the gaps between the barrel HCal and the endcaps. Also shown in fig. 7b is the curve for a hypothetical case where the gaps are completely closed. The flux leakage in this case is then minimal with the stray field about 1 Gauss. This is hypothetical as these gaps are necessary to allow for passage of services to and from the detectors within ePIC and they cannot be completely closed.

Case Studies

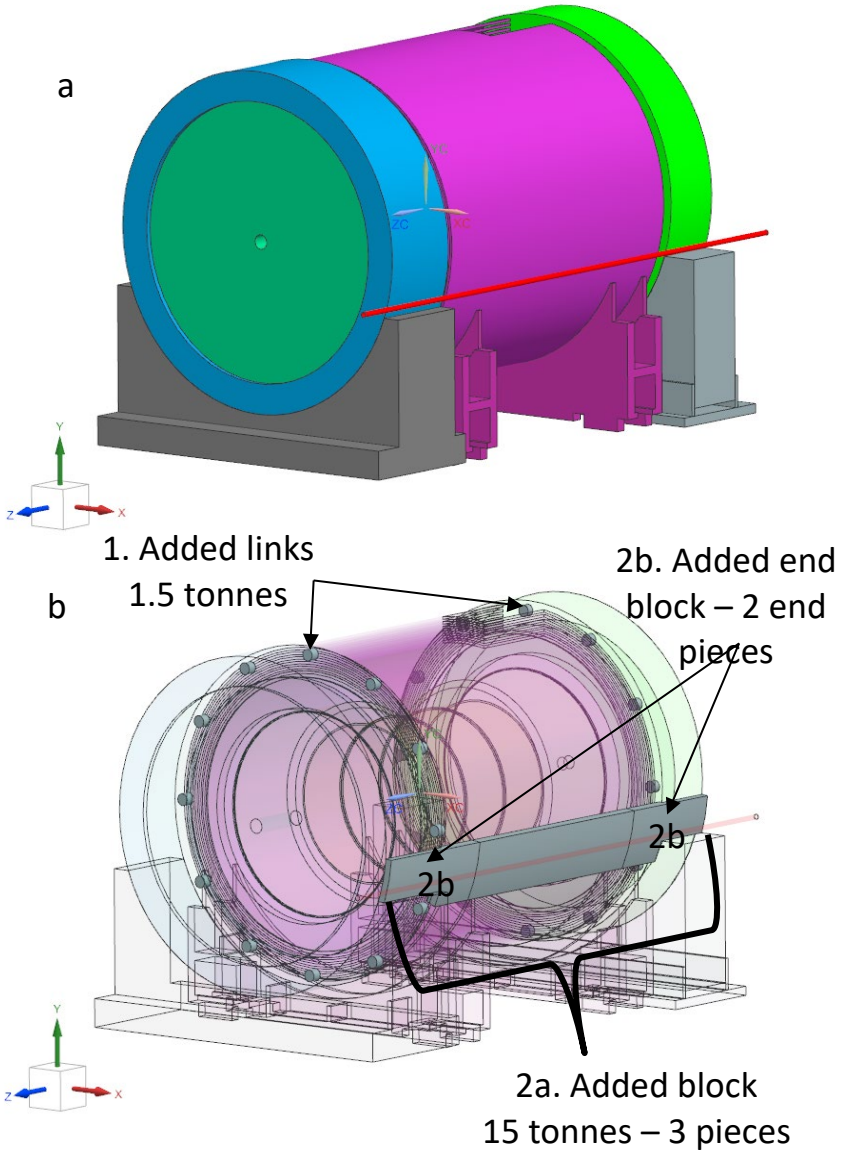

Figure 8 a. Baseline configuration b. Additional steel bodies (opaque) shown with baseline magnetic model (translucent).

To reduce the stray field further, electromagnetic analysis were performed using additional steel shielding elements, which were strategically placed in and around the endcap gaps (Fig. 8b). The goal is to place steel in and around the gaps between the barrel HCal and the endcaps to redirect the field lines away from the RCS beamline. While also limiting the impact on space availability to transfer services to and from the detectors – creating additional complexity.

The general types of steel elements were:

1. Links – Cylindrical bars placed between the barrel and endcap HCal.

   The links are the additional bodies 230 mm cylindrical bodies were created which bridge

the gap between the barrel HCal and the end caps. We have a total of 24 bodies, 12 bodies for each end cap.

2. Block – Annular sector type pipe between the detector and the RCS beamline.

   The block is a pipe with solid annular sector of 20 degrees was created such that it maintained contact with the outer surfaces of the endcaps as well as the barrel shield. This block maintains a 25 mm distance to the RCS beam line. The block has a max thickness of 206.54 mm and a min thickness of 137.54 mm. The block has been divided into 3 pieces and implemented in simulations in two ways:

   a. with the complete block, and
   b. with only the two end pieces denoted as "end blocks" from here on out.

3. RCS tube – Tubular shielding around the RCS.

All the results for cases with different variations of the steel elements are documented in the Appendix and only the significant cases are discussed below.

Discussion

Table 2 and Table 3 summarize the effects of the added steel elements relative to the baseline case. The variation of the magnetic field components along the RCS beamline from -5 m to 5 m is shown in Fig. 9 – 12.

Table 2 Case study summary showing total integrated field and added weight of steel elements.

	Case	B (0,0,0) (T)	∫B.dl (Tm) at RCS line (x=3353, y=-914, z=-5000 to 5000)	Added bodies	Added weight (Tonnes)
1	Baseline	2	0.0187	-	0
2	Baseline+links+Block	2	0.0019	1,2a	16.5
3	Baseline+link+end blocks	2	0.0044	1,2b	7.7
4	Baseline+links	2	0.0124	1	1.5
5	Baseline+block	2	0.0082	2	15
6	Baseline+end blocks	2	0.0111	2b	6.2

Table 3 Case study summary showing stray fields at two-point locations and directional integrated field.

	Case	B (0,0,-5.3 m) (G)	B(0,0,7.4 m) (G)	∫Bx.dl (T-m)	∫By.dl (T-m)	∫Bz.dl (T-m)
1	Baseline	8.83	7.05	-0.0012	-0.0014	0.0091
2	Baseline+links+Block	1.84	0.94	-0.0003	0.0000	0.0013
3	Baseline+link+end blocks	2.69	1.65	-0.0006	0.0001	0.0022
4	Baseline+ links	8.22	3.53	0.0029	-0.0031	0.0051
5	Baseline+block	4.29	3.17	-0.0004	-0.0003	0.0041
6	Baseline+end blocks	5.30	3.94	-0.0013	0.0001	0.0052

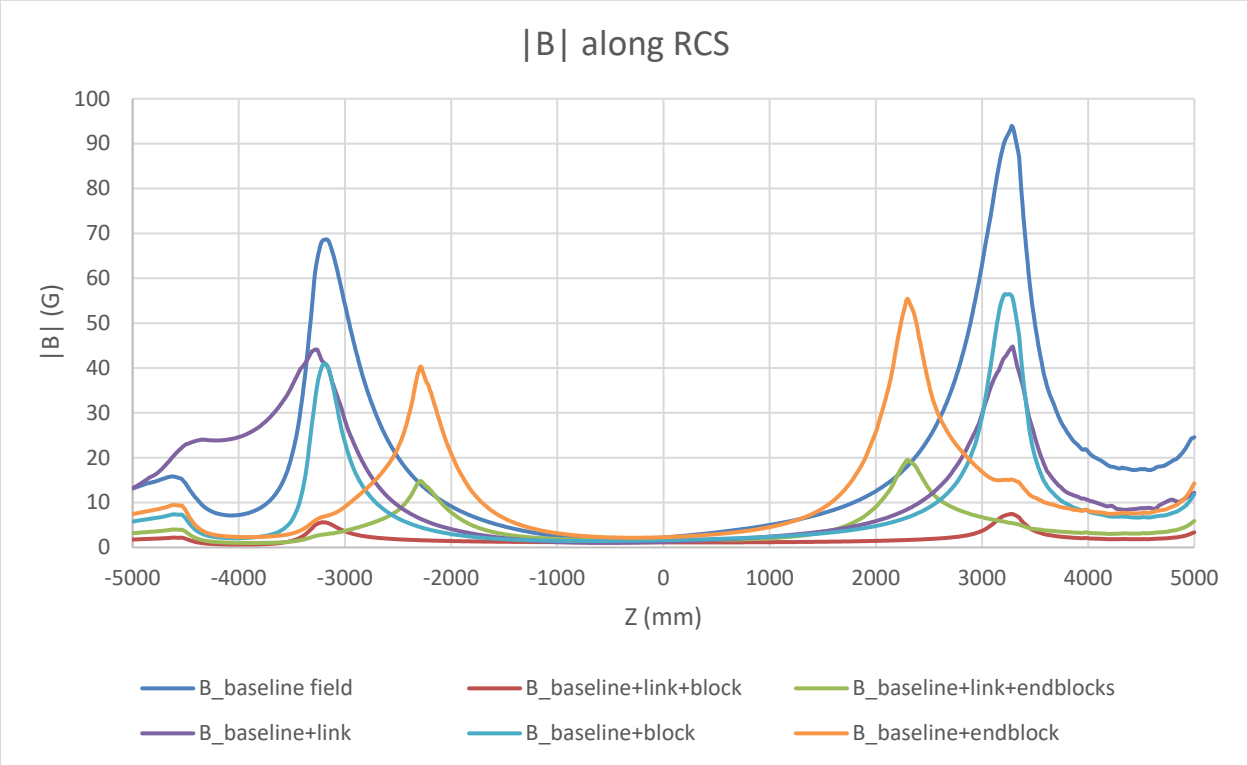

Figure 9 Magnetic field (|B|) comparison along the RCS of the five case studies and the baseline flux return configuration.

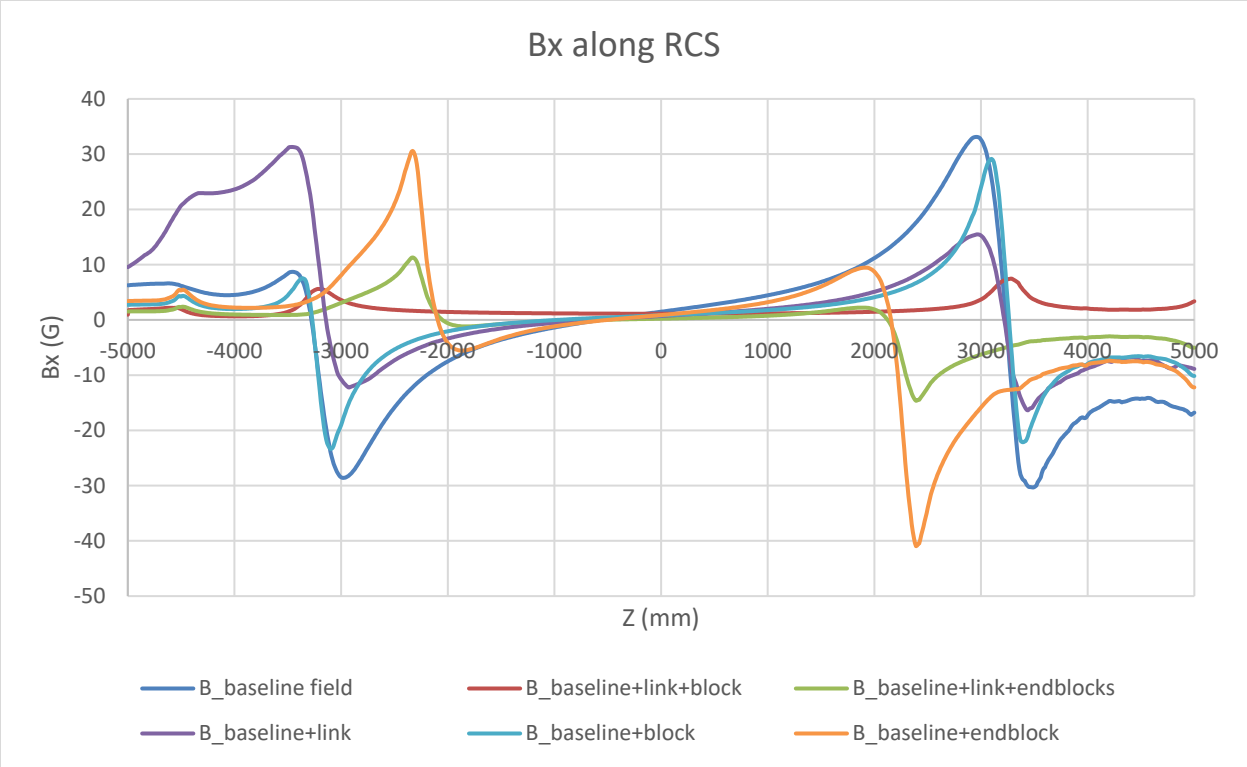

Figure 10 Magnetic field- X component (Bx) comparison along the RCS of the five case studies and the baseline flux return configuration.

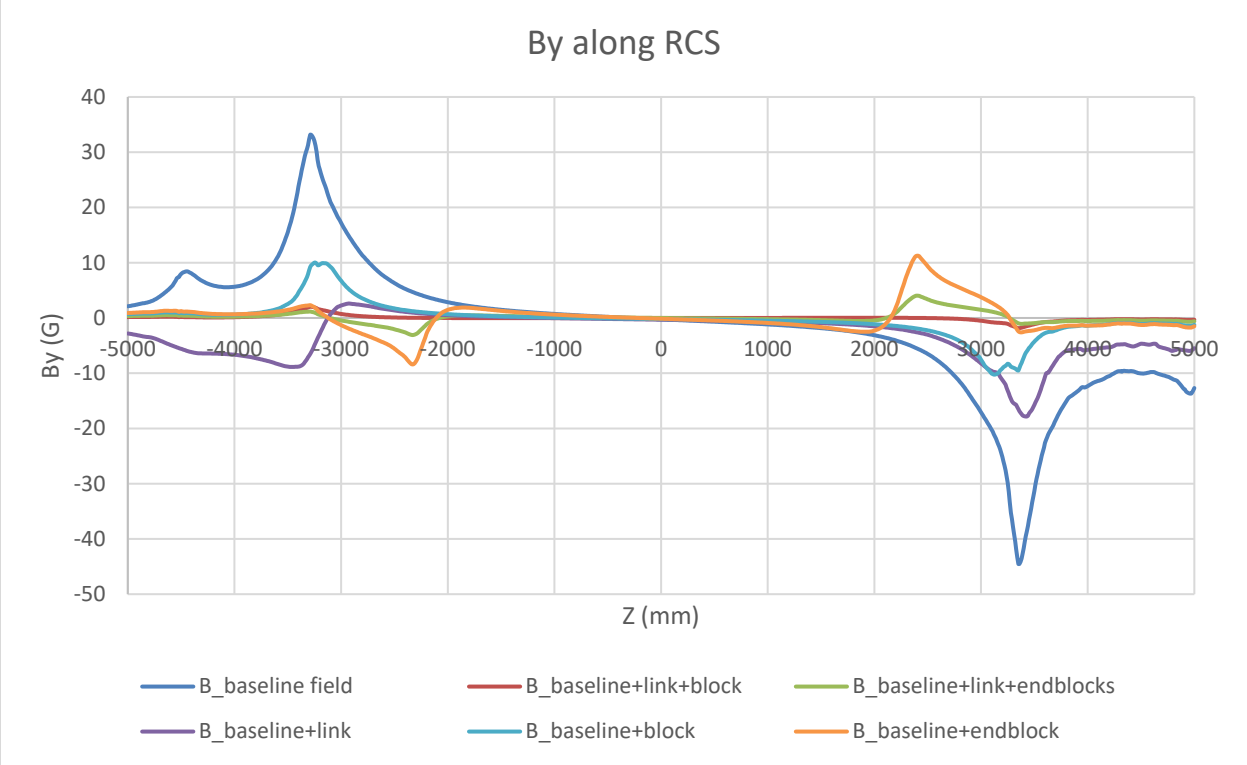

Figure 11 Magnetic field- Y component (By) comparison along the RCS of the five case studies and the baseline flux return configuration.

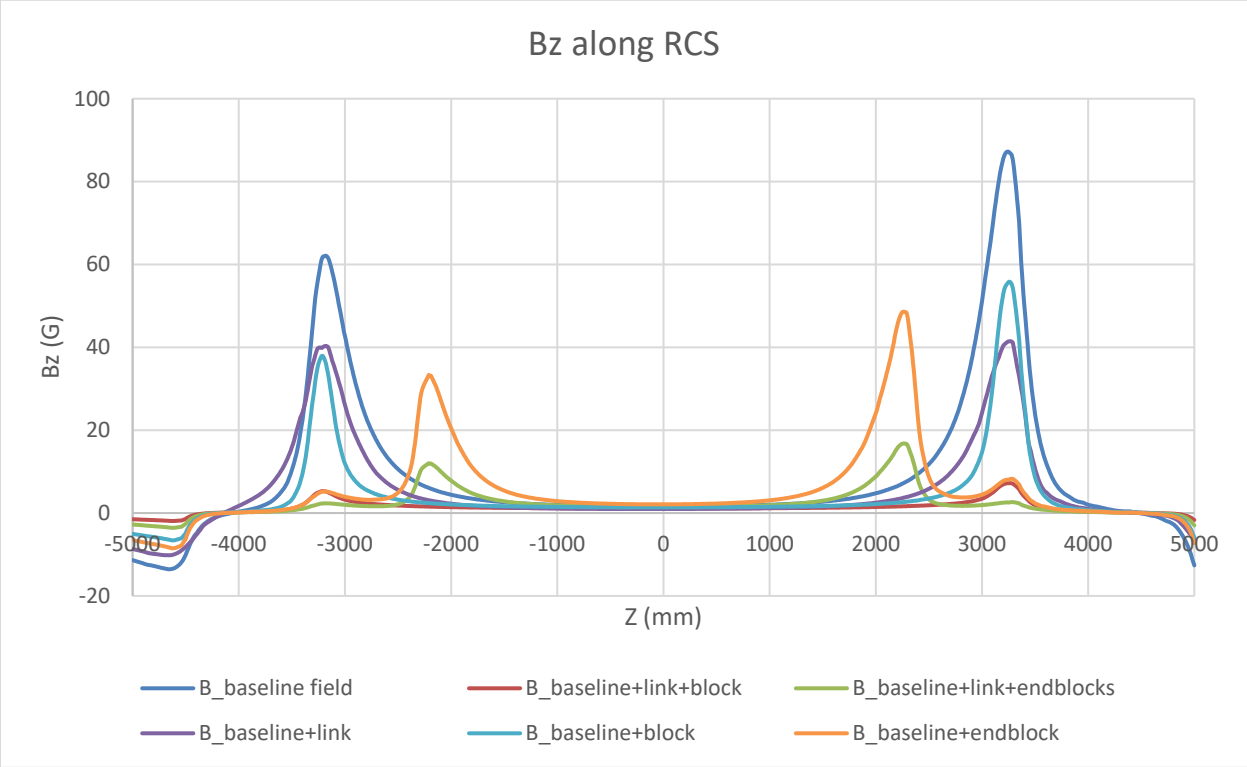

Figure 12 Magnetic field- Z component (Bz) comparison along the RCS of the five case studies and the baseline flux return configuration.

Fig. 13 shows the longitudinal field integral along the RCS for various lengths. The values are low and is tending to zero with increasing length.

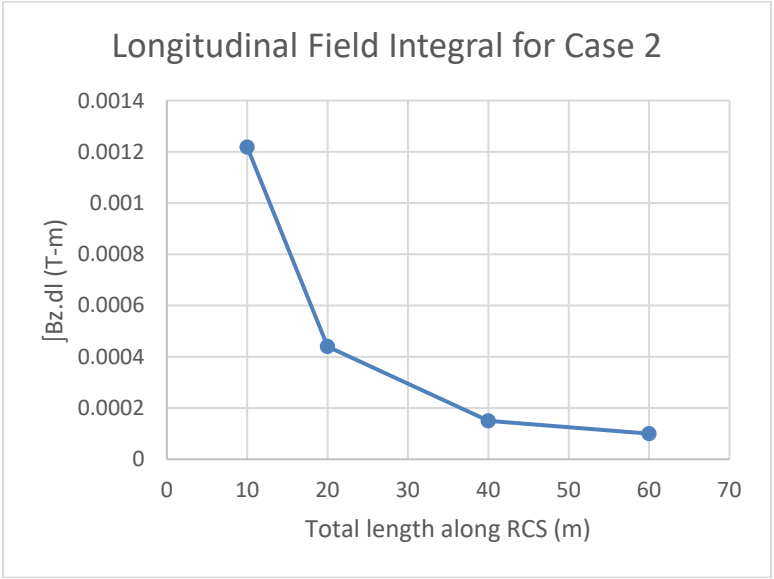

Figure 13 Longitudinal field integral (∫Bz.dl) along the RCS for case 2 in Table 2 and Table 3

Conclusion

The magnetic flux return of the MARCO magnet is mainly absorbed by a combination of flux return steel and steel in the barrel and forward hadronic calorimeters acting as flux return. The magnetic fringe fields are primarily caused by unavoidable gaps between the barrel detector and end caps needed to provide space for services to come out. We investigated ways to minimize these fringe fields for strategic locations, at the space of the first focusing magnets and along the RCS beam line. The magnetic stray field along the RCS was minimized using strategically placed steel shielding elements. Electromagnetic analysis were performed to characterize the total integrated field for the various cases of steel shielding elements. The added steel elements are placed between the barrel HCal and Endcap gaps (links) and between the ePIC detector and the RCS beamline. The block and the RCS tube are in the tight space between the ePIC detector and the RCS beamline while the links are in the gaps between the barrel steels.

The baseline case showed a total integrated field of 0.018 Tm which was optimized to a $1/10^{th}$ using additional 16.5 tonnes of steel to 0.0019 Tm (Fig. 9). First links (24 cylindrical bodies of 230 mm diameter) were added into the gaps, which reduced the total integrated field to 0.0124 Tm ($2/3^{rd}$ of the base line). This was further reduced to 0.0019 Tm with the addition of the 15.5 tonne block (200 mm thick pipe piece) between ePIC and the RCS beamline. The block makes a significant reduction in the field – it reduces the baseline field to ½ - 0.008 -Tm by itself without links. A smaller version of the block called the “end blocks” (which are half the weight of the block) were studied and those in conjunction with links reduce the baseline field by $2/10^{th}$ to 0.004 Tm. Newer studies show that the total integral field limit on the RCS beamline could be higher – 0.0293 Tm longitudinal integral field and 0.024 Tm transverse integral field [4] (0.007 Tm total field integral was considered at the beginning of this document). Fig.13 is a quick sanity check that confirms TOSCA simulations are converging as the field integral tends to zero with increasing length.

The studies show conclusively that the stray fields can be reduced significantly by the addition of one or more from all the three proposed type of shield elements. The selection of the type of shield elements will depend on the complexity involved in the final application. The final solution will have to be evaluated as the engineering design of the detector, the RCS, and the support structures mature.

Acknowledgement

The present work is the outcome of a collaboration between Jefferson Lab and CEA, Saclay. Special thanks to Valerio Calvelli (CEA, Saclay) for sharing the workload and performing electromagnetic simulations in TOSCA.

References

[1] *Opera-3D 2022SP2 Reference Manual*; Dassault Systèmes UK Ltd.: Kidlington, UK, 2018

[2] Renuka Rajput-Ghoshal, *EIC-Central Detector Solenoid HCal Position and Size 1.0*

[3] Elke Aschenauer, *Email to Renuka Rajput-Ghoshal*, Feb 2022

[4] Vahid Ranjbar, *RCS Field Tolerances at IP6/IP8,* Feb 2024

Appendix

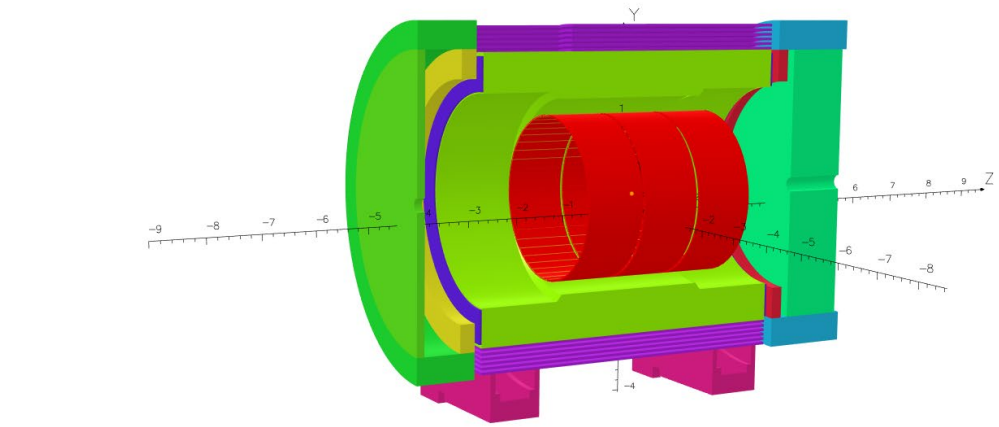

Figure 14 Baseline Geometry (Baseline A) for all the cases discussed in the appendix

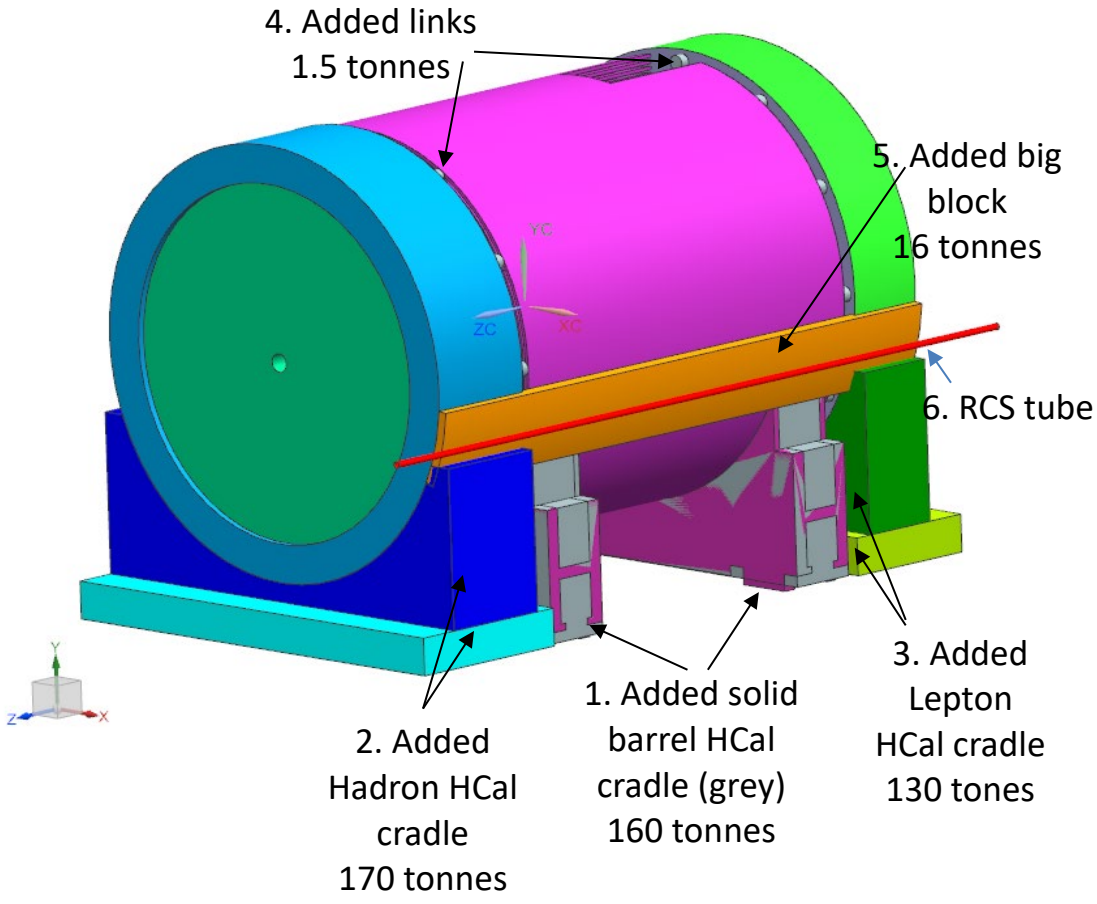

Figure 15 Additional steel options with the baseline case as shown in Fig. 7. Steel element numbering only applicable to the appendix content

Figure 16 Tube around RCS beamline with rings

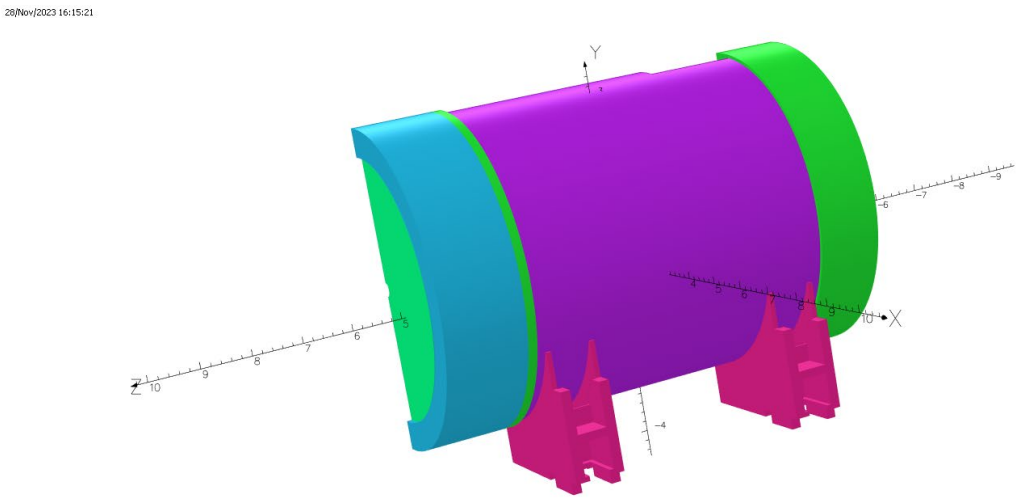

Figure 17 Baseline A with gaps closed with additional steel – not a realistic solution

Fig 8 shows the summary of added steel elements to Baseline A. Below are the details of the additions:

1. HCal Cradles – Solid cradles were developed with the same outer dimensions of the existing cradles.
2. Hadron HCal cradles – Solid cradles were developed from preliminary detailed design for the Hadron end cap.
    a. JLab approximation
    b. Updated BNL version
3. Lepton HCal cradles – Solid cradles were developed from preliminary detailed design for the Hadron end cap.
    a. JLab approximation
    b. Updated BNL version
4. Links – Cylindrical bodies were created which bridge the gap between the barrel shields and the end caps. Total 24 bodies, 12 bodies for each end cap.
    a. Smaller links – 50 mm diameter
    b. Bigger links – 230 mm diameter
5. Big Block – A pipe with solid annular sector of 20 degrees was created such that it maintained contact with the outer surfaces of the endcaps as well as the barrel shield. This block maintains a 25 mm distance to the RCS beam line. The block has a max thickness of 206.54 mm and a min thickness of 137.54 mm.

6. RCS Tube – Low Carbon steel that surrounds the RCS beamline (x=3353, y=-914, z=-5000 to 5000).
    a. A tube of 170 mm outer diameter (OD) and 102 mm inner diameter (ID).
    b. Tube in 6a but with flanges of OD 190 mm, 15 mm thick spaced every 400 mm on the tube.

Table 4 Summary of Results

Case	Simulation details	B (0,0, 0) (T)	B (0,0,-5300) (G)	B(0,0,7400) (G)	B (3400,0, 0) (G)	∫B.dl (Tm) at RCS line (x=3353, y=-914, z=-5000 to 5000)	Added bodies	Added weight (Tonnes)
1[+]	Baseline A (Fig. 7)	2	15.33	10.34	2.34	0.029	-	0
2[+]	Baseline A + HCal cradle	2	9.8	6.64	1.88	0.018	2a,3a	300
3[x]	Gap closed (Fig. 10)	2	1.05	0.28	0.6	0.00078	NA	NA
4	Baseline A + smaller links in the gap	2	14.88	10.01	2.29	0.022	4a	0.05
5	Baseline A+ Bigger and solid cradles	2	9.61	6.55	1.82	0.018	1,2a,3a	400
6	Baseline A + Bigger link	2	7.53	5.04	1.15	0.014	4b	1.5
7*	Baseline A + Bigger link+ big block at the back	2	2.25	1.10	1.01	0.003147	4b,5	17.5
8	Baseline A + big block at the back	2	6.68	4.43	1.52	0.014	5	16
9	Baseline A + tube around RCS	2	15.19	10.0	2.31	0.01	6a	1.1
10	Baseline A + tube and rings around RCS	2	14.95	9.91	2.27	0.0088	6b	1.2
11*	Baseline A + tube and rings around RCS + HCal Cradle	2	12.84	7.70	1.86	0.0055	6b,2a,3a	301

12	Baseline A + Bigger and solid cradles+ bigger Links	2	5.394	3.376	1.06	0.00998	1,2a,3a, 4b	401.5
13	Baseline A + Simplified cradle for endcaps+ bigger Links	2	8.22	3.53	1.1	0.0127	2b,3b, 4b	301.5
14*	Baseline A + tube and rings around RCS + simplified HCal Cradle	2	12.3	8.4	2.2	0.0062	6b, 2b,3b	301
15*	Baseline A + tube and rings around RCS + simplified HCal Cradle+links	2	6.8	4.2	0.25	0.0024	6b, 2b,3b, 4b	302.5

+ Values are along the XZ plane at X=3.4 m, Z= -4.5 m to 5 m

X Unrealistic steel placement, not a valid solution – lowest stray field possible

* Cases satisfy field requirement